Preface

This semi-annual report describes our progress during the period from September 1988 to February 1989. There are four separate tasks described in this report. Although, some of these tasks are interdependent, their reports should be read independently. That is, figure and reference numbering is consecutive only within the description of a given task. As can be expected, the progress report on each task is brief. The reader is expected to refer to the detailed reports or papers referenced in the progress reports.

TABLE OF CONTENTS

TABLE OF CONTENTS - (Cont.)

Task 1: A FINITE ELEMENT CONJUGATE GRADIENT FFT METHOD FOR SCATTERING

Period Covered: September 1988 - February 1989

Investigators: J.D. Collins and J.L. Volakis

Task Description:

This task calls for the development of an innovative iterative technique particularly suited for simulating large size scatterers. In constrast to traditional techniques, the proposed approach demands an FFT algorithm one order lower than the dimensionality of the modeled structure, in addition to having an $O(N)$ memory requirement. It is, therefore, expected to allow the simulation of practical size geometries without restrictions on the geometrical and material properties of the structure.

A goal during this year's effort is to develop a demonstration model of the method. In particular, a two-dimensional implementation of the approach will be developed. A finite element mesh generator will also be developed in conjunction with this implementation.

1 Background

There exists a continuing need and interest in the simulation of three dimensional configurations. Present matrix inversion techniques have excess storage demands and are therefore limited to small size geometries. A recent emphasis in the use of iterative techniques is due to the aforementioned limitation. The most popular among iterative techniques is the Conjugate Gradient (CG) method which ensures convergence in a finite number of steps. Of particular importance, though, in the use of iterative techniques are the advantages realized when they are combined with the Fast Fourier Transform (FFT). Since the unknown source distribution is found by iteration, the usual convolution integrals can be evaluated using the standard FFT at each iteration, thus eliminating a need for generating and storing a square matrix. The storage demands in a CGFFT solution are therefore reduced to $O(N)$, a rather substantial reduction from the $O(N^2)$ usually required for a solution involving a matrix inversion. Unfortunately, the storage reduction is achieved at the expense of computational efficiency, particularly when computations are desired for many excitations. As a result, there is a pressing need for the development of computationally efficient algorithms.

Over the past two years [1,2], at the University of Michigan we have developed new simulation approaches particularly suited for the implementation of the CGFFT algorithm. A major part of our study also included the generation of new efficient FFT algorithms when employed in conjunction with the CG method, and these have already been provided to some industrial organizations.

Nevertheless, present approaches of analysis such as those considered previously

have relied on the use of a three-dimensional FFT in the simulation of an arbitrary geometry of the same dimensionality. Specifically, the scattering configuration is enclosed in a rectangular box which usually determines the size of the three-dimensional FFT. A solution is then obtained by imposing boundary conditions associated with the scattering structure and in conjunction with the radiation condition imposed at the surface of the box. The last is usually satisfied implicitly by employing what is usually referred to as the boundary integral method, which substantially complicates the analysis. An alternative to the boundary integral approach is to increase the size of the enclosing box and employ a direct application of the radiation condition. The last is, however, highly undesirable since it requires the introduction of far more additional unknowns.

As we have recently shown when employing vector-concurrent FFT algorithms [3], most of the computational demands in a CGFFT solution are consumed in the implementation of the FFT. This work calls for an innovative iterative methodology that demands an FFT algorithm one order lower than the dimensionality of the structure. That is, the proposed algorithm requires the use of only two-dimensional FFTs in simulating a three-dimensional structure, implying a substantial improvement in computational efficiency. This is achieved by combining the (highly successful in mechanical and structural applications) Finite Element Method (FEM) with the usual CGFFT. Briefly, by employing the FEM procedure, the fields at the scatterer's location are transferred to the surface of the rectangular enclosing box using finite element interpolation (a linear interpolation), a rather simple and efficient task. As a result, all cumbersome integrations over the irregular scattering structure are eliminated, and the only integrals which result in the entire implementation are those called for in the application of the boundary integral method. These are, however, only over the surface of the enclosing box and are, as a result, easily computed with a two-dimensional FFT. The resulting system, satisfying the scatterer's boundary conditions and the radiation condition, implicit in the application of the boundary integral method is a matrix involving the fields within and on the surface of the enclosing box. Inherent to the application of the FEM, the matrix is highly diagonal and thus easily stored, except for that part of the matrix involving the (integration of the) surface fields. However, since the last are computed with the FFT, the storage demand is again reduced from $O(N^2)$ to $O(N)$. Therefore, the storage requirement is maintained at $O(N)$ as in the traditional CGFFT implementation, but the algorithm now requires only a two-dimensional FFT (rather than a three-dimensional one) for the treatment of arbitrary three-dimensional scatterers.

During the first year of this effort, we are only considering a two-dimensional implementation of the method.

2 Theory

Consider a perfectly conducting body illuminated by an incident field

$$\overline{\phi}^{inc} = \hat{z}\phi^{inc} = \hat{z}e^{jk\rho\cos(\theta-\theta_o)} \tag{1}$$

at an angle θ_o, as indicated in fig. 1. ϕ may represent either E_z for $E-$polarization or H_z for $H-$polarization. An $e^{j\omega t}$ time dependence has been assumed (and suppressed).

To analyze the fields scattered by the given structure, two rectangular boxes are employed to enclose the structure. The rectangular shape of the enclosures is necessary to allow subsequent use of the FFT. Also, by allowing the outer box (Γ_a) to be only one cell larger than the inner (Γ_b) the singularity associated with the Green's function is completely avoided. Inside the outer boundary Γ_a, the Finite Element Method (FEM) is employed to transfer the field from the object's boundary to Γ_b. An integral equation is then formed to relate the field on Γ_a to that on Γ_b

2.1 Finite Element Analysis

Interior to Γ_a, we are required to solve the Helmholtz equation, or equivalently, employ the variational technique [4] by minimizing the functional

$$F = \iint_{R_I} \left\{ \frac{1}{\mu_r(\overline{r})} \nabla\phi \cdot \nabla\phi^{a*} - k_o^2 \epsilon_r(\overline{r}) \phi\phi^{a*} \right\} ds - \int_{\Gamma_a} \phi^{a*} \nabla\phi \cdot \hat{\boldsymbol{n}}_a dl \tag{2}$$

for E-polarization, and

$$F = \iint_{R_I} \left\{ \frac{1}{\epsilon_r(\overline{r})} \nabla\phi \cdot \nabla\phi^{a*} - k_o^2 \mu_r(\overline{r}) \phi\phi^{a*} \right\} ds - \int_{\Gamma_a} \phi^{a*} \nabla\phi \cdot \hat{\boldsymbol{n}}_a dl \tag{3}$$

for H-polarization, where $k_o^2 = \omega^2 \mu_o \epsilon_o$, $\hat{\boldsymbol{n}}_a$ is the outward normal from Γ_a and $*$ denotes complex conjugation. Furthermore, ϕ^a is the solution to the adjoint problem and is identically equal to ϕ for lossless media. The region between Γ_a and Γ_c can be subdivided into M linear triangular elements having a total of N nodes. The field within this region (to be referred to as the FE region) can then be expressed as

$$\phi(x,y) = \sum_{e=1}^{M} \sum_{i=1}^{3} N_i^e(x,y) \phi_i^e \tag{4}$$

where $N_i^e(x,y)$ is the shape function of the e^{th} element, and ϕ_i^e is the unknown field at node i of the e^{th} element. A partial discretization is shown in fig. 2, and it should be noted that Γ_a is allowed to be a single cell away from Γ_c. It can easily be shown that the system

$$A\phi = \psi \tag{5}$$

can be derived by minimizing F in either (2) or (3) and substituting (4) into resulting expression. An expanded form of (5) can be written as

$$\begin{bmatrix} A_{aa} & A_{ab} & 0 & 0 \\ A_{ba} & A_{bb} & A_{bI} & 0 \\ 0 & A_{Ib} & A_{II} & A_{Ic} \\ 0 & 0 & A_{cI} & A_{cc} \end{bmatrix} \begin{bmatrix} \phi_a \\ \phi_b \\ \phi_I \\ \phi_c \end{bmatrix} = \begin{bmatrix} \psi_a \\ 0 \\ 0 \\ 0 \end{bmatrix} \tag{6}$$

where the subscripts a, b and c are associated with the nodes on contours Γ_a, Γ_b and Γ_c, respectively, while the nodes internal to the region between contours Γ_b and Γ_c are denoted by the subscript I. As a result, ϕ_a, ϕ_b, ϕ_I and ϕ_c denote the field quantities at the respective nodes. Note that for $E-$polarization, the boundary condition on the body is satisfied by setting $\phi_c = 0$, which reduces the size of the system. For $H-$polarization, however, the boundary condition is satisfied naturally through the variational technique.

The quantity ψ_a in the right hand side of the system (6) is specific to the boundary condition satisfied on Γ_a. For Γ_a at infinity, this would, of course, be the radiation condition. Since this is not the case, the first row of (6) is replaced by the boundary integral considered next.

2.2 Boundary Integral Formulation

The solution to the Helmholtz equation for the region outside of Γ_a is given by the integral equation expression

$$\phi(\overline{r}) = \phi^{inc}(\overline{r}) - \oint_{\Gamma_b} \{G(\overline{r},\overline{r}_b)\left[\hat{\boldsymbol{n}}_b \cdot \nabla\phi(\overline{r}_b)\right] - \phi(\overline{r}_b)\left[\hat{\boldsymbol{n}}_b \cdot \nabla G(\overline{r},\overline{r}_b)\right]\}\, dl_b \tag{7}$$

which satisfies the radiation condition. We evaluate this expression on the boundary Γ_a to provide us with the remaining boundary condition. The Green's function for this problem is

$$G(\overline{r},\overline{r}') = -\frac{j}{4}H_o^{(2)}(k|\overline{r}-\overline{r}'|) \tag{8}$$

where $\overline{r}$ and $\overline{r}'$ are the usual observation and source position vectors, respectively. Additionally,

$$|\overline{r}-\overline{r}'| \;=\; \sqrt{(x-x')^2+(y-y')^2} \tag{9}$$

where (x, y) are the observation coordinates, and (x', y') are the source coordinates.

The integral in (7) can be written as a summation of four integrals over each side of the contour Γ_b as

$$\begin{aligned}
\phi(\overline{r}) = \phi^{inc}(\overline{r}) \;&-\; \left\{\int_{\Gamma_{b1}} \left[G(\overline{r},\overline{r}_b)\frac{\partial}{\partial y}\phi(\overline{r}_b) - \phi(\overline{r}_b)\frac{\partial}{\partial y}G(\overline{r},\overline{r}_b)\right] dl_{b1}\right.\\
&+\; \int_{\Gamma_{b2}} \left[-G(\overline{r},\overline{r}_b)\frac{\partial}{\partial x}\phi(\overline{r}_b) + \phi(\overline{r}_b)\frac{\partial}{\partial x}G(\overline{r},\overline{r}_b)\right] dl_{b2}\\
&+\; \int_{\Gamma_{b3}} \left[-G(\overline{r},\overline{r}_b)\frac{\partial}{\partial y}\phi(\overline{r}_b) + \phi(\overline{r}_b)\frac{\partial}{\partial y}G(\overline{r},\overline{r}_b)\right] dl_{b3}\\
&+\; \left.\int_{\Gamma_{b4}} \left[G(\overline{r},\overline{r}_b)\frac{\partial}{\partial x}\phi(\overline{r}_b) - \phi(\overline{r}_b)\frac{\partial}{\partial x}G(\overline{r},\overline{r}_b)\right] dl_{b4}\right\}
\end{aligned} \tag{10}$$

where $\Gamma_b = \Gamma_{b1} + \Gamma_{b2} + \Gamma_{b3} + \Gamma_{b4}$ as implied by fig. 2. Approximating the normal derivatives of ϕ as

$$\frac{\partial}{\partial x}\phi(x_b, y') = \frac{1}{\Delta}\left[\phi(x_a, y') - \phi(x_b, y')\right] \tag{11}$$

$$\frac{\partial}{\partial y}\phi(x', y_b) = \frac{1}{\Delta}\left[\phi(x', y_a) - \phi(x', y_b)\right] \tag{12}$$

where Δ is the displacement of Γ_a from Γ_b (see fig. 2), and substituting into (10), we obtain a typical expression for (10)

$$\begin{aligned}
\phi(x, y_{a1}) &= \phi^{inc}(x, y_{a1}) \\
&- \left\{ -\int_{x_{b4}}^{x_{b2}} \left[\frac{1}{\Delta}G(x - x', y_{a1}, y_{b1})\phi(x', y_{a1}) - \left(\frac{1}{\Delta} + \frac{\partial}{\partial y}\right) G(x - x', y_{a1}, y_{b1})\phi(x', y_{b1})\right] dx' \right. \\
&- \int_{y_{b3}}^{y_{b1}} \left[\frac{1}{\Delta}G(x, x_{b2}, y_{a1}, y')\phi(x_{a2}, y') + \left(-\frac{1}{\Delta} + \frac{\partial}{\partial x}\right) G(x, x_{b2}, y_{a1}, y')\phi(x_{b2}, y')\right] dy' \\
&+ \int_{x_{b2}}^{x_{b4}} \left[\frac{1}{\Delta}G(x - x', y_{a1}, y_{b3})\phi(x', y_{a3}) + \left(-\frac{1}{\Delta} + \frac{\partial}{\partial y}\right) G(x - x', y_{a1}, y_{b3})\phi(x', y_{b3})\right] dx' \\
&+ \left. \int_{x_{b3}}^{x_{b1}} \left[\frac{1}{\Delta}G(x, x_{b4}, y_{a1}, y')\phi(x_{a4}, y') - \left(\frac{1}{\Delta} + \frac{\partial}{\partial x}\right) G(x, x_{b4}, y_{a1}, y')\phi(x_{b4}, y')\right] dy' \right\}
\end{aligned} \tag{13}$$

for observation along the contour/boundary Γ_{a1}. The first and third terms of (13) are convolutions and may, therefore, be evaluated via the FFT. The remaining terms are not in convolution form and must, therefore, be solved directly. Since their integrals do not cross any singularities, they can be evaluated via a simple midpoint integration.

For convenience, (10) may be written as

$$\phi_a = \phi_a^{inc} - L_{aa}\phi_a - L_{ab}\phi_b \tag{14}$$

or alternatively as

$$(L_{aa} + I)\phi_a + L_{ab}\phi_b = \phi_a^{inc} \tag{15}$$

Replacing the first row in (6) by (15) now yields

$$\begin{bmatrix} L_{aa}+I & L_{ab} & 0 & 0 \\ A_{ba} & A_{bb} & A_{bI} & 0 \\ 0 & A_{Ib} & A_{II} & A_{Ic} \\ 0 & 0 & A_{cI} & A_{cc} \end{bmatrix} \begin{bmatrix} \phi_a \\ \phi_b \\ \phi_I \\ \phi_c \end{bmatrix} = \begin{bmatrix} \phi_a^{inc} \\ 0 \\ 0 \\ 0 \end{bmatrix} \tag{16}$$

which is amenable to a numerical solution via the CGFFT method.

3 Current Status and Future Plans

The theoretical analysis associated with this task has been completed, and a computer code has been written. At present, most of the code has been debugged, and it is expected that a working version will be available by the end of March. At that time, optimizations in memory and CPU time will be pursued. Also, before continuing with a three-dimensional implementation of the approach, generalizations to non-metallic and composite structures will be considered.

During this period, a mesh generator was also developed and interfaced with the main code.

A detailed report relating to this task will be written after completion of the code.

References

[1] T.J. Peters, "Computation of Scattering by Planar and Non-planar Plates using the Conjugate Gradient FFT Method", Ph.D. Thesis, The University of Michigan, Ann Arbor, MI, 1988.

[2] K. Barkeshli and J.L. Volakis, "Improving the Convergence of the Conjugate Gradient FFT Method Using Subdomain Basis Functions", accepted to *IEEE Trans. on Antennas and Propagat.*

[3] K. Barkeshli and J.L. Volakis, " A Vector-Concurrent Application of a Conjugate Gradient FFT Algorithm to EM Radiation and Scattering", 3rd biennial IEEE conference on electromagnetic field computation, Dec. 1988.

[4] M.V.K. Chari and P.P. Silvester, Eds., *Finite Elements in Electrical and Magnetic Field Problems*, London, New York: Wiley, 1980.

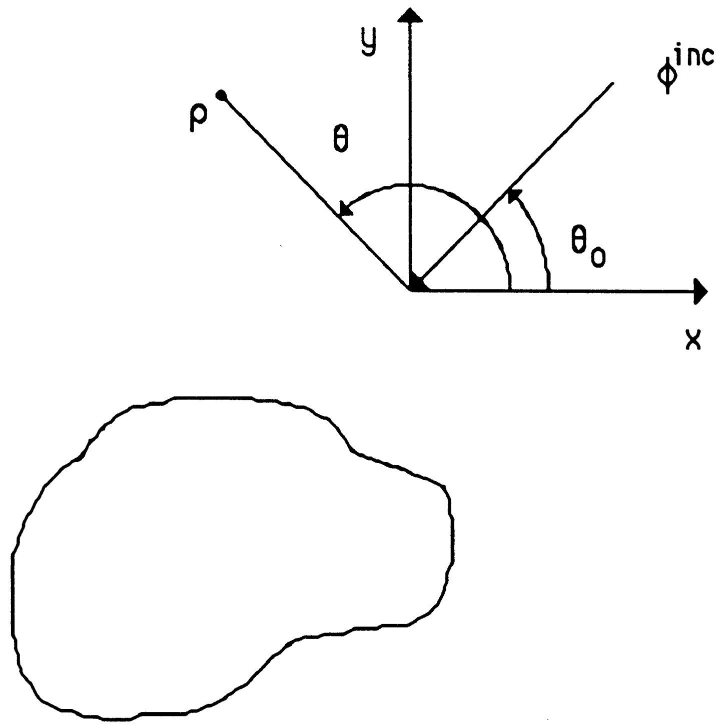

Figure 1. Cross section of a perfectly conducting cylinder.

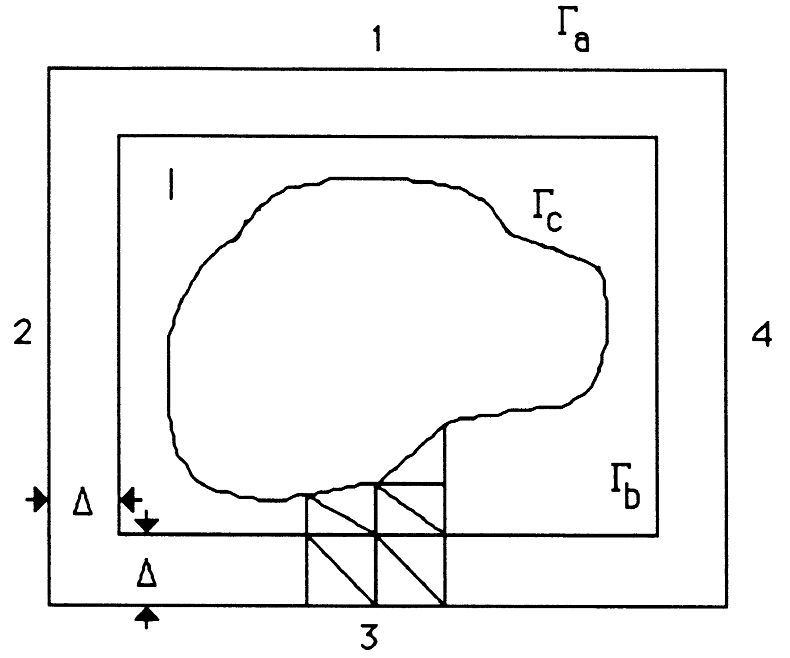

Figure 2. Cylinder enclosed in a rectangular box and partial discretization.

Task 2: DEVELOPMENT OF GENERALIZED IMPEDANCE BOUNDARY CONDITIONS

Period Covered: September 1988 - February 1989

Investigators: J.L. Volakis, T.B.A. Senior and J.-M. Jin

Task Description:

The purpose of this task is to develop improved boundary conditions allowing an accurate simulation of thick coatings and layers. Boundary conditions are proposed which involve involve higher order derivatives leading to a non-local characterization of the coating. They promise solutions to new diffraction problems and more efficient numerical simulation by eliminating a need to sample within the dielectric.

1 Background

The use of non-metallic materials, possibly in the form of a non-uniform or multilayer coating applied to a metallic substrate, has made necessary the development of methods for simulating material effects in scattering. This is important in the analytical treatment of canonical geometries and also for the efficient generation of numerical solutions.

A possible approach is to employ approximate boundary conditions [1], and the impedance (or Leontovich) boundary condition [2] has been widely used for this purpose. But this condition allows only one degree of freedom through the single surface impedance assumed, and there are limits to the surface properties that can be simulated in this manner. The inclusion of higher order derivatives of the field components on the surface increases the flexibility , and leads to a hierarchy of boundary conditions as discussed in this paper. The first order version is equivalent to the standard impedance condition. An example of the second order version was developed by Weinstein [3] and in [4],[5] to simulate thin dielectric layers with and without a metal backing.

Under this task we explore the suitability of higher order or generalized impedance boundary conditions (GIBCs) originally proposed by Karp and Karal [8] to study surface waves supported by dielectric coatings. General methodologies are developed for generating the conditions and their accuracy is examined as a function of the order of the condition.

2 Progress

All work intended under this task has essentially been completed and the report "Derivation and Application of a Class of Generalized Impedance Boundary Conditions - II" was recently submitted to NASA (University of Michigan Radiation Laboratory technical report 025921-T-1). A paper based on this report has also been submitted for publication. Below is a summary contained in this report.

For the sake of simplicity consider a surface at $y = 0$ where the region $y < 0$ is occupied by a laterally homogeneous material, but possibly inhomogeneous in depth. To replace the presence of this surface a boundary condition is proposed at $y = 0$ having the form

$$\begin{aligned} \sum_{m=0}^{M} \frac{a_m}{(ik)^m} \frac{\partial^m}{\partial y^m} E_y &= 0 \\ \sum_{m=0}^{M'} \frac{a'_m}{(ik)^m} \frac{\partial^m}{\partial y^m} H_y &= 0 \end{aligned} \qquad (1)$$

where a_m and a'_m are constants specific to the properties of the modeled surface. A major portion of the report is devoted to the development of approaches leading to the derivation of these constants for given configurations of interest. Some of these are:

(i) The reflection coefficients implied by (1) are

$$\begin{aligned} R(\phi) &= -\frac{\sum_{m=0}^{M}(-1)^m a_m \sin^m \phi}{\sum_{m=0}^{M} a_m \sin^m \phi} \\ R(\phi) &= -\frac{\sum_{m=0}^{M'}(-1)^m a'_m \sin^m \phi}{\sum_{m=0}^{M'} a'_m \sin^m \phi} \end{aligned} \qquad (2)$$

corresponding to the E_y and H_y components, respectively. Thus, if an analytical expression of the reflection coefficient is available, it can be expanded as in (2), leading to the identification of the constants.

(ii) If the reflection coefficients are not availiable but the geometry of the profile is known, a Taylor series expansion can be employed to transfer the fields to the surface of the profile leading again to the identification of the constants. This procedure is essentially equivalent to (i).

(iii) The reflection coefficients (2) can be seen to be associated with poles. Given the surface wave poles of the structure, the constants may be chosen to recover the poles.

(iv) In the case where the profile's inner cross section is not known or not conforming to analysis, measured or numerical data of the reflection coefficients can be used to determine the constants by curve fitting.

In addition to the determination of the constants, of importance is the location of their application and an approach was introduced for transferring the location where they are enforced. Finally, to generalize (1) for application to curved surfaces, they must be written in terms of tangential derivatives. In doing so, a duality condition must be satisfied as discussed in the report.

As an illustration of the application of the GIBCs (1), the constants were determined for two specific geometries shown in figures 1 and 2. These correspond to a uniform and a three-layer metal backed coating, respectively. A fourth order condition was derived for the uniform coating and its accuracy was examined by comparing its implied reflection coefficient with the exact. As shown in figure 3, the maximum layer thickness that can be modeled with the fourth order condition is at least 0.25 free space wavelengths with a maximum of 2 degrees error in phase. In case of lossy coatings, the simulation of thicker coatings is possible.

3 Future Goals

The above applications illustrated that the generalized boundary conditions provide an acceptable simulation of multilayered and/or inhomogeneous coatings. Of primary interest in the immediate future is to employ these conditions in obtaining analytical and numerical solutions to problems of interest. Analytically, it is important to determine diffraction coefficients that can be incorporated into general purpose GTD codes and we have already begun to do this [9],[10]. In fact, Task 3 is devoted to this subject. Unfortunately, Weiner-Hopf analyses with the GIBCs bring new difficulties because of the inherent nonuniqueness of the generated solutions. As a result, a major part of Task 3 has been devoted to resolving this issue.

In the case of numerical applications, the GIBCs offer advantages of simplicity and efficiency (because they eliminate a need to sample within the structure) without compromising accuracy. Task 4 addresses this application which also has not been without difficulties. As noted later, the GIBCs must be supplemented with additional conditions at abrupt material terminations. Also, care must be exercised in a numerical treatment of the higher order derivatives.

References

[1] T. B. A. Senior, "Approximate Boundary Conditions," IEEE Transactions on Antennas and Propagation, Vol. AP-29, pp. 826-829, 1981.

[2] T. B. A. Senior, 'Impedance Boundary Conditions for Imperfectly Conducting Surfaces," Appl. Sci. Res., Vol. 8(B), pp.418-436

[3] A. L. Weinstein, The Theory of Diffraction and the Factorization Method, Golem Press: Boulder, CO., 1969.

[4] J. L. Volakis and T. B. A. Senior, "Applications of a Class of Generalized Boundary Conditions to Scattering by a Metal-Backed Dielectric Half-Plane," Proc. IEEE, May 1989.

[5] T. B. A. Senior and J. L. Volakis, "Sheet Simulation of a Thin Dielectric Layer," Radio Sci., vol. 22, pp. 1261-1271, 1987.

[6] B. Engquist and A. Majda, "Absorbing Boundary Conditions for the Numerical Simulation of Waves," Math. Comput., vol. 31, pp. 629-651, 1977.

[7] L. N. Trefethen and L. Halpern, "Well-Posedness of One-Way Equations and Absorbing Boundary Conditions," Math. Comp., vol. 47, pp. 421-435, 1986.

[8] S. N. Karp and F. C. Karal, Jr., "Generalized Impedance Boundary Conditions with Applications to Surface Wave Structures," in Electromagnetic Wave Theory, Part 1, ed. J. Brown, pp. 479-483, Pergamon: New York, 1965.

[9] J. L. Volakis and T. B. A. Senior, "Diffraction by a Thin Dielectric Half Plane," IEEE Trans. Antennas Propagat., AP-35, pp. 1483-1487, 1987.

[10] J. L. Volakis, "High Frequency Scattering by a Material Half-Plane and Strip," Radio Sci., 23, pp. 450-462, May-June 1988.

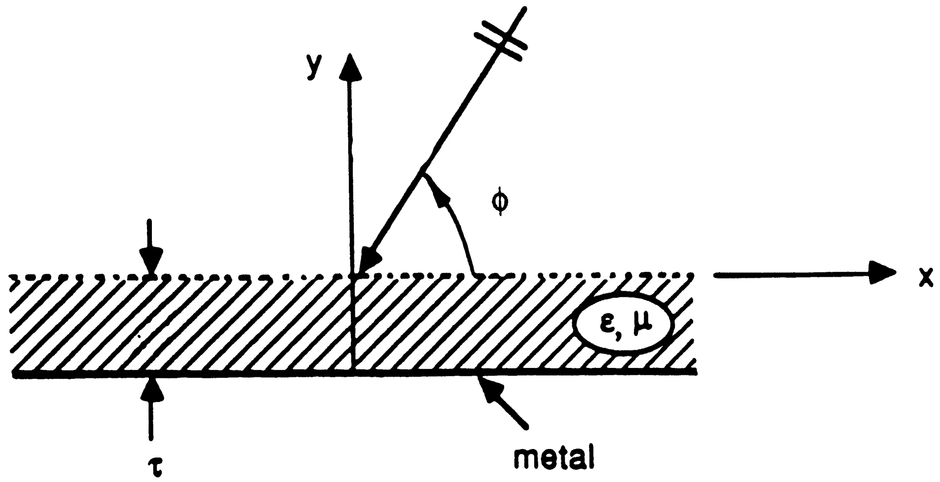

Figure 1

Fig. 1. Geometry of a metal-backed dielectric layer.

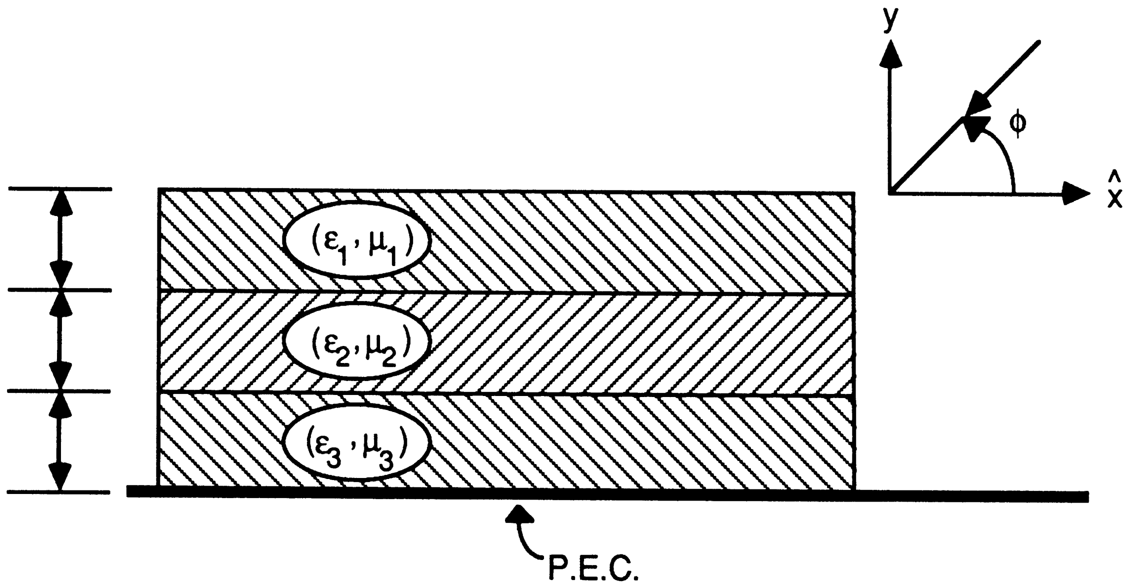

Fig. 2. Geometry of a three layer metal-backed coating.

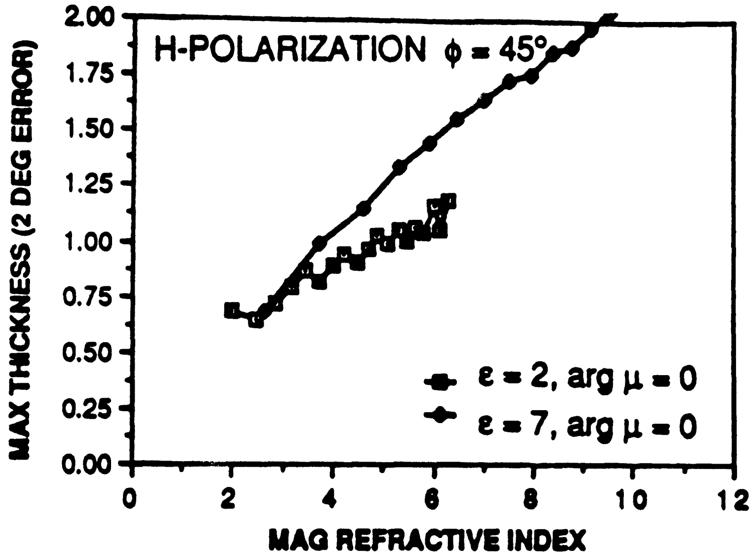

(a)

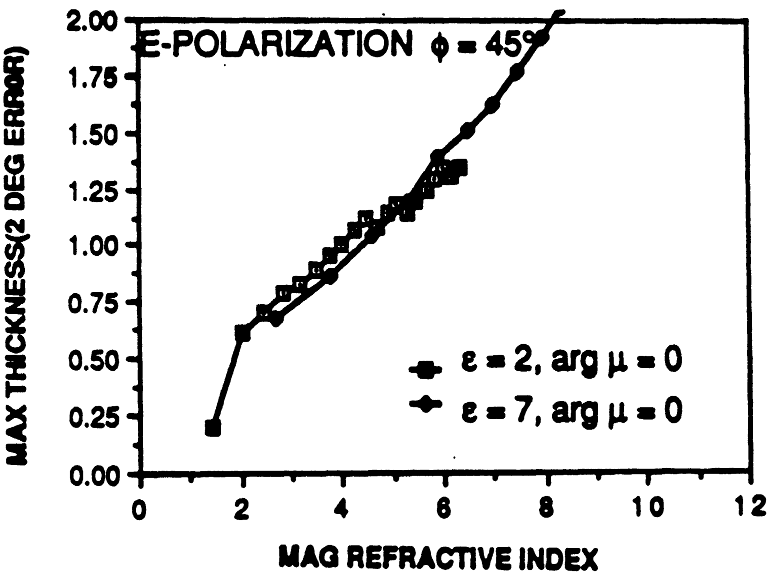

(b)

Fig. 3. Maximum allowed thickness vs $\sqrt{\mu\varepsilon}$ for a metal-backed dielectric layer modelled using the 4th order boundary conditions at $y = \tau+$, with a 2-degree phase (and/or 2 percent amplitude) error. Curves shown are for $\varepsilon = 2$ and $\varepsilon = 7$ with $\phi = 45$ degrees: (a) H-polarization, (b) E-polarization.

Task 3: ANALYTICAL SOLUTIONS WITH GENERALIZED IMPEDANCE BOUNDARY CONDITIONS (GIBCs)

Period Covered: September 1988 - February 1989

Investigators: M. A. Ricoy and J. L. Volakis

Task Description:

This task involves the use of higher order boundary conditions (see Task 2) to generate new solutions in diffraction theory. In particular, diffraction coefficients will be developed for dielectric/magnetic layers and metal-dielectric junctions which are often encountered on airborne vehicles as terminations of coatings and conformal antennas. Solutions for both polarizations will be developed for fairly thick junctions and versatile computer codes will be written and tested.

1 Background

In modeling the scattering properties of an arbitrary body, one generally focuses on the presence of abrupt discontinuities. A particular class of discontinuity whose occurence among man-made structures is commonplace is the junction of dissimilar materials. In general, the characterization of these junctions in an exact manner (e.g. [1],[2]) is a difficult problem. Usually the results obtained are not in closed form and are thus extremely cumbersome to apply. On the other hand, considerable success has been realized through the modeling of simple junctions with the impedance boundary condition [3],[4],[5],[6], which is in fact a GIBC of first order. The obtained solutions offer the advantage of being extremely simple and easy to implement relative to their exact counterparts. However, their validity is restricted to the case where the material is either very thin electrically or else opaque. This suggests the possibility of using higher order boundary conditions to model simple junctions in the hope of relaxing these restrictions, while maintaining a relative simplicity over exact methods.

Higher order boundary conditions were first introduced by Kane and Karp [7], who subsequently employed a second order GIBC to compute the diffraction of a radiowave propagating over a half-space with a discontinuity in dielectric constant [8]. Jones [9] later considered surface wave diffraction by a semi-infinite slab on a ground plane using an infinite order GIBC. More recent work has centered upon the material half-plane [10],[11],[12],[13],[14] and the coated wedge [15],[16]. Unfortunately, these investigations have revealed two major shortcommings of employing GIBCs in conjunction with function-theoretic techniques:

- the obtained solution is not necessarily reciprocal with respect to angle of incidence and observation, and
- the obtained solution may not be unique.

In [13],[14], and [16], the authors were cognizant of the first item above and were able to obtain solutions that satisfied reciprocity. Nevertheless, imposing this condition did not make their solutions unique.

2 Progress Summary and Future Plans

The goal of the work associated with this task is to generate new analytical solutions via the use of GIBCs. The fulfillment of this goal involves several subtasks, firstly, the derivation of diffraction coefficients for material-metallic junctions and possibly material-material junctions, with major consideration given to the resolution of the uniqueness problem described above. The second subtask is the development of computer codes based on the obtained analytical solutions and the demonstration of their versatility/validity through the computation of numerical results. The final subtask is the generation of a detailed report and journal papers.

In accomplishing the above objectives, we chose to study material junctions on a ground plane. First, infinite order GIBCs were developed for a material layer on a ground plane through examination of the exact reflection coefficient. Finite order approximations to these were then obtained for the case of a low contrast material (accuracy increases as layer thickness decreases) and a high contrast material (accuracy increases as the index of refraction increases).

Subsequently, these GIBCs were employed to treat the problem of a material insert in a perfectly conducting ground plane (figure 1). The problem was formulated with a dual integral equation approach [17] in conjunction with the generalized scattering matrix technique [18]. A convenient by-product of this method is the solution of the diffraction from a grounded material slab with a truncated upper plate (figure 2). Since little extra work is required, simultaneous solutions were obtained for the the exact case as well as the GIBC case to illustrate the accuracy of the GIBC solution. We note that for this situation, both the exact and GIBC solutions were unique.

Another discontinuity of interest is that shown in figure 3. By formulating the problem in terms of the dual integral equation approach as before, an analytical solution was obtained. But, unlike the solution for the material-metallic junction, the one associated with the material-material junction was non-unique. Currently, we are comparing the resulting spectra with those obtained for the material insert and truncated upper plate solutions. It appears that when one side of the material-material junction solution is perfectly conducting, the resulting expression for the diffracted field incorporates the solutions associated with the material-metallic junction and of the truncated upper plate (figure 2). This is extremely significant in establishing a fundamental cause of non-uniqueness stemming from a lack of sufficient conditions to characterize the junction below the surface.

The computer codes associated with the above analytical solutions are currently under development and the final report is being written. It is expected that these remaining tasks will be completed in approximately a month and a half.

Future work will focus on employing the diffraction coefficients developed herein to characterize microstrip structures which contain a multiplicity of scattering centers. Hence, a major effort will be placed on developing multiple scattering methodologies which are numerically efficient. Subsequently, these results will be extended to the case of skew incidence. Finally, a three-dimensional implementation will be considered through the use of the equivalent current concept [19].

References

[1] C. M. Angulo, "Diffraction of surface waves by a semi-infinite dielectric slab," IRE Transactions on Antennas and Propagation, Vol. AP-5, pp. 100-109, January 1957.

[2] K. Aoki and K. Uchida, "Scattering of a plane electromagnetic wave by two semi-infinite dielectric slabs," The Transactions of the IECE of Japan, Vol. 62-B, No. 12, pp. 1132-1139, 1979.

[3] A. F. Kay, "Scattering of a surface wave by a discontinuity in reactance," IRE Transactions on Antennas and Propagation, Vol. AP-7, pp. 22-31, January 1959.

[4] R. Tiberio and G. Pelosi, "High frequency scattering from the edges of impedance discontinuities on a flat plane," IEEE Transactions on Antennas and Propagation, Vol. AP-31, No. 4, pp. 590-596, July 1983.

[5] P. H. Pathak and R. G. Rojas, "A UTD analysis of the em diffraction by an impedance discontinuity in a planar surface," Journal of Wave-Material Interaction, Vol. 1, pp. 16-37, January, 1986.

[6] R. G. Rojas, "Weiner-Hopf Analysis of the em diffraction by an impedance discontinuity in a planar surface and by an impedance half-plane," IEEE Transactions on Antennas and Propagation, Vol. AP-36, No. 1, pp. 71-83, January 1988.

[7] J. Kane and S. N. Karp, "An accurate boundary condition to replace transition condition at dielectric-dielectric interfaces," Institute of Mathematical Sciences Division of E.M. Research, New York University, New York, N. Y., Research Report EM-153, May 1960.

[8] J. Kane and S. N. Karp, "Radio propagation past a pair of dielectric interfaces," Institute of Mathematical Sciences Division of E.M. Research, New York University, New York, N. Y., Research Report EM-154, May 1960.

[9] W. R. Jones, "A new approach to the diffraction of a surface wave by a semi-infinite grounded dielectric slab," IEEE transactions on Antennas and Propagation, Vol. AP-12, pp. 767-777, November, 1964.

[10] I. Anderson, "Plane wave diffraction by a thin dielectric half-plane," IEEE Transactions on Antennas and Propagation, Vol. AP-27, No. 5, pp. 584-589, September 1979.

[11] R. G. Rojas, "A uniform GTD analysis of the em diffraction by a thin dielectric/ferrite half-plane and related configurations," Ph.D. Dissertation, The Ohio State University, Department of Electrical Engineering, Columbus, Ohio, 1985.

[12] A. Chakrabarti, "Diffraction by a dielectric half-plane," IEEE Transactions on Antennas and Propagation, Vol. AP-34, No. 6, pp. 830-833, June 1986.

[13] J. L. Volakis and T. B. A. Senior, "Diffraction by a thin dielectric half-plane," IEEE Transactions on Antennas and Propagation, Vol. AP-35, No. 12, De-

cember 1987.

[14] J. L. Volakis, "High frequency scattering by a thin material half-plane and strip," Radio Science, Vol. 23, No. 3, pp. 450-462, May-June 1988.

[15] J. M. L. Bernard, "Diffraction by metallic wedge covered with a dielectric material," Journal of Wave Motion, Vol. 9, pp. 543-561, 1987.

[16] J. L. Volakis and T. B. A. Senior, "Diffraction by a coated wedge using second and third order generalized boundary conditions," Radiation Laboratory Report 388967-8-T, The University of Michigan, Ann Arbor, Michigan, September 1988.

[17] P. C. Clemmow, "A method for the exact solution of a class of two-dimensional diffraction problems," Proc. Roy. Soc. A, Vol. 205, pp. 286-308, 1951.

[18] J. R. Pace and R. Mittra, "Generalized scattering matrix analysis of waveguide discontinuity problems," Proc. Symp. Quasi-Optics, Vol. 14, Brooklyn, N.Y., Polytechnic Inst. of Brooklyn Press, pp. 177-197, 1964.

[19] R. G. Kouyoumjian, "The general theory of diffraction and its applications," in Numerical and Asymptotic Techniques in Electromagnetics, R. Mittra, Ed., New York, Springer-Verlag, 1975.

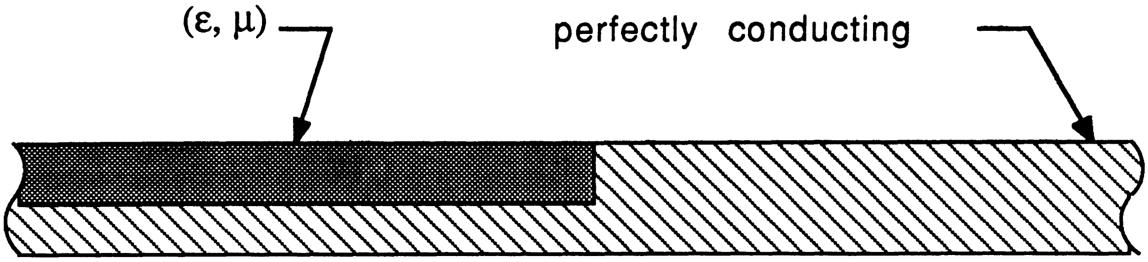

Figure #1. Material slab recessed in a perfectly conducting ground plane.

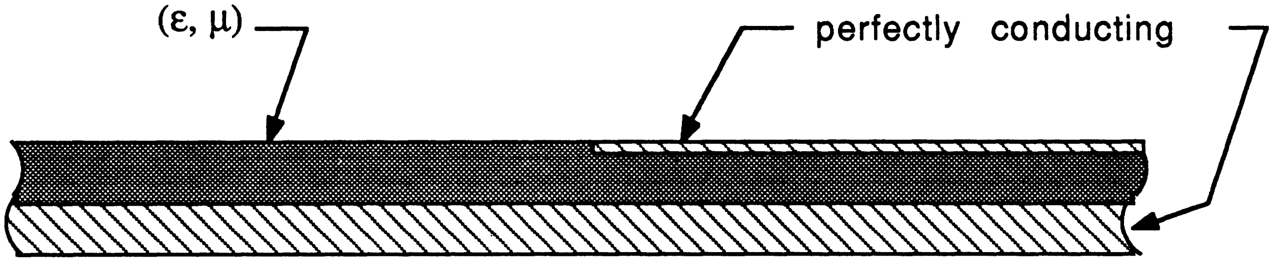

Figure #2. Grounded material slab with truncated upper plate.

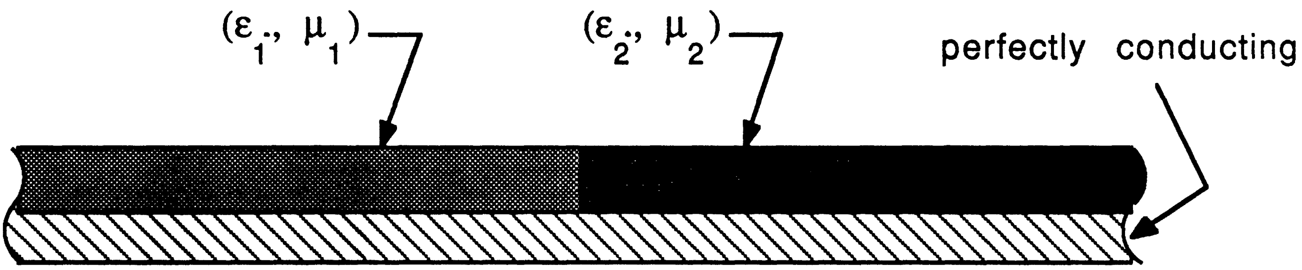

Figure #3. Material discontinuity in a grounded material slab.

Task 4: NUMERICAL IMPLEMENTATION OF GENERALIZED IMPEDANCE BOUNDARY CONDITIONS

Period Covered: September 1988 - February 1989

Investigators: K. Barkeshli and J. L Volakis

Task Description: This task deals with the development of numerical solutions based on the generalized impedance boundary conditions (GIBCs). The purpose of this task is to demonstrate the efficiency and simplicity associated with GIBC solutions as well as examine their limitations.

1 Background

Traditionally, the standard impedance condition (SIBC) [1] has been employed to simulate thin material layers on perfectly conducting objects. As is well known, however, the SIBC provides limited accuracy and is particularly applicable to lossy and/or high contrast dielectrics. This is primarily because it cannot model the polarization current components that are normal to the dielectric layer. As a result, the SIBC has been found to be best suited for near normal incidence, unless the coating's material properties are such that it limits penetration within the material.

The SIBC is a first order condition in that its definition involves a single normal derivative of the component of the field normal to the modeled surface. Recently [2], however, a class of boundary conditions were proposed whose major characteristic is the inclusion of higher order derivatives (along the direction of the surface normal) of the normal field components. These were originally introduced by Karp and Karal [3] and Weinstein [4] to simulate surface wave effects, but have been found to be rather general in nature. In fact, they can be employed to simulate any material profile with a suitable choice of the (constant) derivative coefficients. Appropriately, they are referred to as generalized impedance boundary conditions (GIBCs) and can be written either in terms of tangential or normal derivatives provided a duality condition is satisfied [2]. Unlike the SIBC they offer several degrees of freedom and allow an accurate prediction of the surface reflected fields at oblique incidences. This was demonstrated in [2] for the infinite planar surface formed by a uniform dielectric layer on a ground plane. It was found that the maximum coating or layer thickness that can be simulated accurately with a given GIBC was analogous to the highest derivative included in the condition.

Task 3 dealt with analytical solutions using the GIBCs. Under this task, we examine numerical solutions based on the GIBCs. It is found that integral equations based on the GIBCs are amenable to a conjugate gradient FFT solution having an $O(N)$ memory requirement.

2 Progress

A detailed report describing our progress during this period was written and submitted to the sponsor. The report is entitled "TE Scattering by a Two-dimensional Groove in a Ground Plane" (University of Michigan Radiation Laboratory report 025921-2-T). A summary of the report follows.

3 Report Summary

An application of a third order generalized boundary condition (GIBC) to scattering by a two-dimensional dielectrically filled cavity was considered (see figures 1 and 2). In the process of examining the accuracy of the GIBC, an exact solution was developed and a solution based on the standard impedance boundary condition (SIBC) was examined. An analytical comparison of the integral equation based on the SIBC with the exact revealed the well known limitations of the SIBC formulation (see figure 3). It was concluded that the SIBC integral equation will, at most, generate an average of the actual current distribution provided the groove is very shallow.

The GIBC integral equation was found easier to implement. Furthermore, unlike the exact integral equation, it was amenable to a conjugate gradient FFT solution and is, thus, attractive for three dimensional implementations. It was found to predict the correct current behavior reasonably well away from the terminations of the groove, particularly for lossy dielectric fillings (see figure 4). However, the inadequacy of the GIBC formulation near the groove terminations proved problematic. The GIBC conditions needed supplementation in these regions and several approaches were examined to correct this deficiency. Our inital hope was that the addition of filamentary currents at the edges would provide the required correction as was already done in the case of an isolated thin dielectric layer. This approach, however, was not found suitable for the subject geometry. Instead, the incorrect currents near the groove terminations were replaced with those computed via the exact integral equations. Specifically, the currents computed via the GIBC formulation away from the groove termination were employed in the exact integral equation to generate a small 4x4 or a 6x6 matrix for the currents in the vicinity of the terminations. This was referred to as a hybrid exact-GIBC approach and was found to provide a reasonably good simulation (see figure 6) of the lossy dielectric fillings at all angles of incidence and observation. In case of lossless and low contrast dielectrics, the simulation was adequate for groove depths up to 3/20 of a wavelength.

References

[1] T. B. A. Senior, "Approximate Boundary Conditions," IEEE Trans. Antennas and Propagat., Vol. AP-29, pp. 826-829, 1981.

[2] T. B. A. Senior and J .L. Volakis, "Derivation and Application of a Class of Generalized Impedance Boundary Conditions," accepted in IEEE Trans. Antennas and Propagat.; see also University of Michigan Radiation Laboratory report 025921-1-T.

[3] S. N. Karp and Karal, Jr., "Generalized Impedance Boundary Conditions with Application to Surface Wave Structures," in Electromagnetic Wave Theory, part 1, ed. J. Brown, pp. 479-483, Pergamon: New York, 1965.

[4] A. L. Weinstein, The Theory of Diffraction and the Factorization Method, Golem Press: Boulder, Co., 1969.

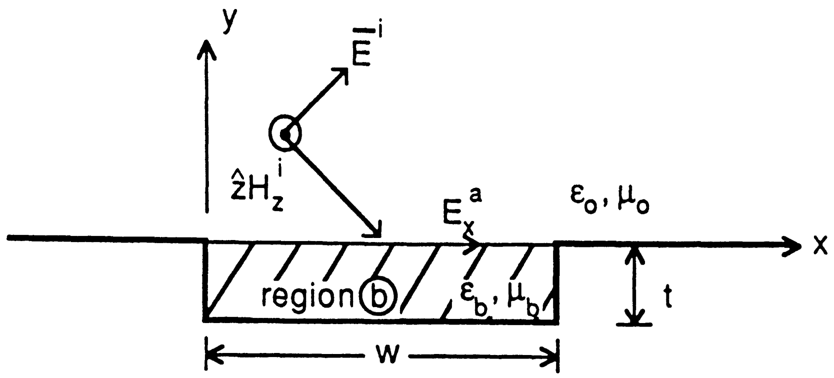

Fig. 1. Geometry of the rectangular groove in a ground plane

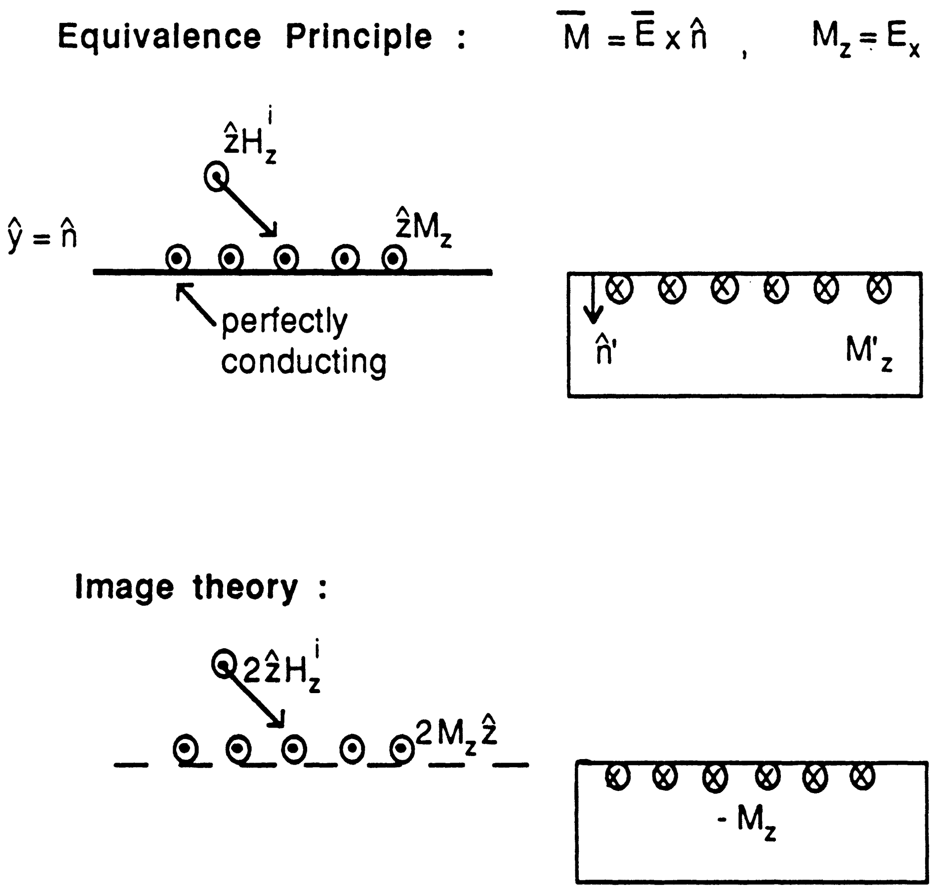

Fig. 2. Illustration of the application of equivalence and image theory.

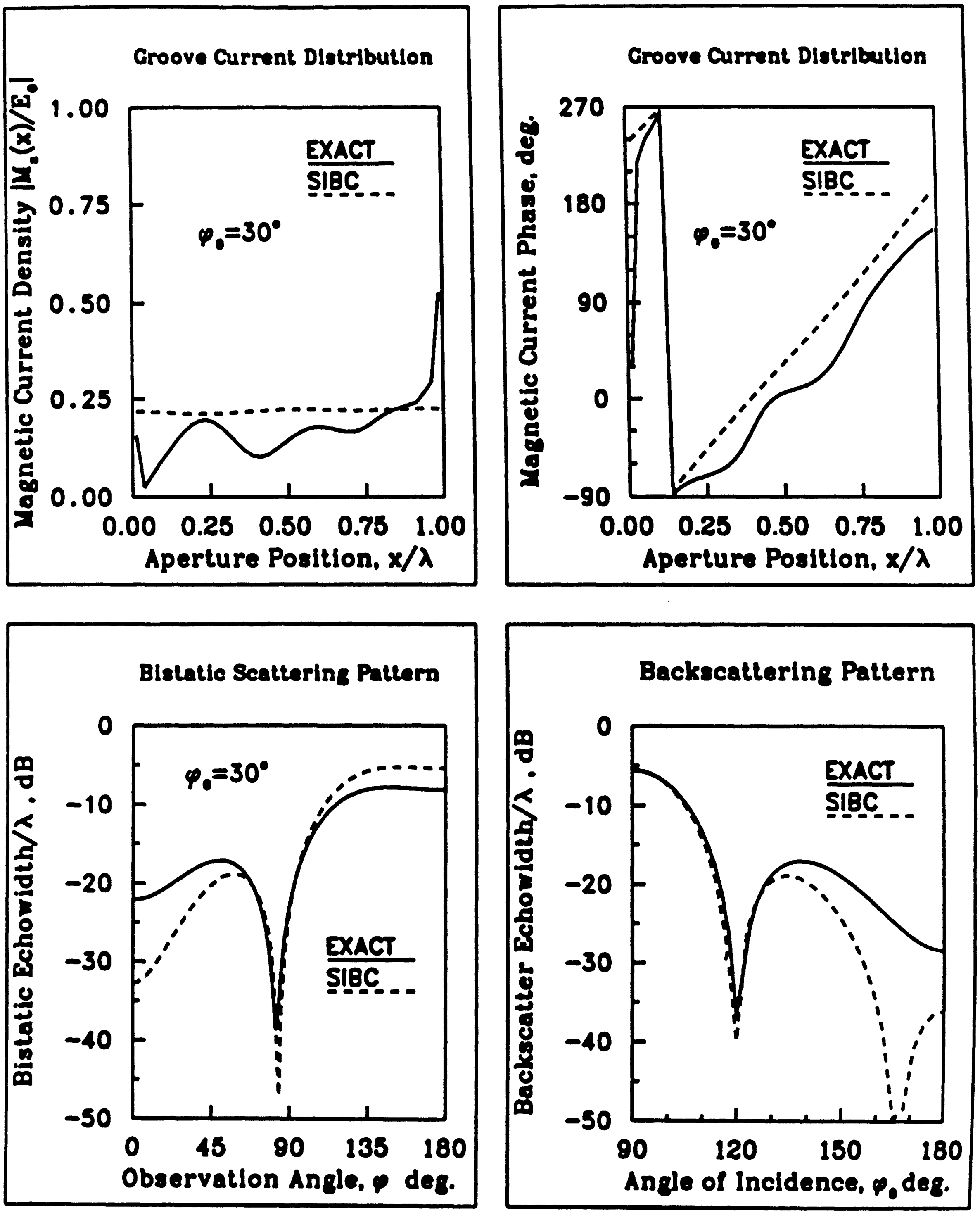

Fig. 3 Comparison of results for scattering from a groove obtained by the exact and the SIBC formulations; groove width w=1λ, depth h=0.2λ, ε_r=7.0−j1.0, μ_r=1.

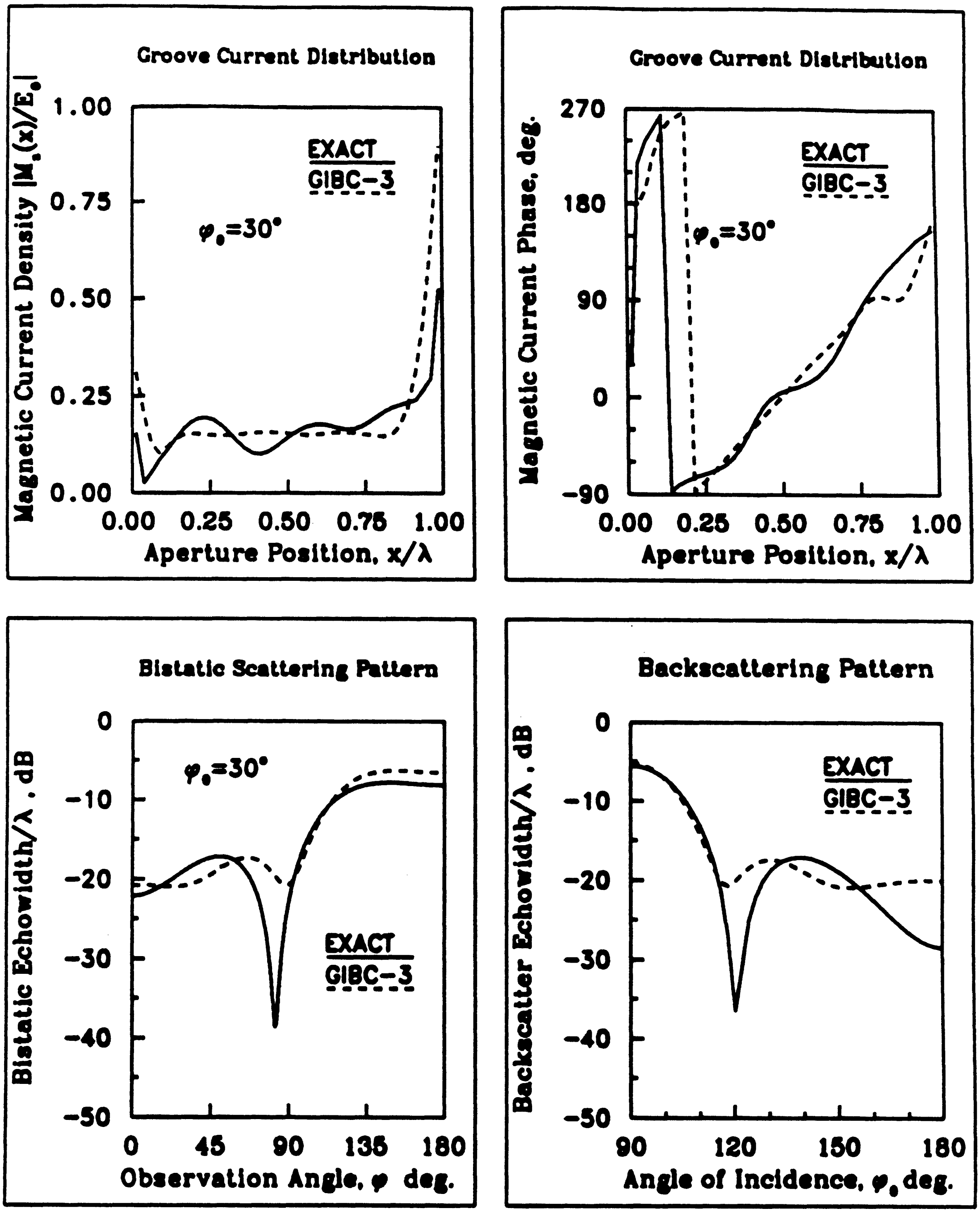

Fig. 4 Comparison of results for scattering from a groove obtained by the exact and the third order GIBC formulations; groove width $w=1\lambda$, depth $t=0.2\lambda$, $\varepsilon_b=7.0-j1.0$, $\mu_b=1$.

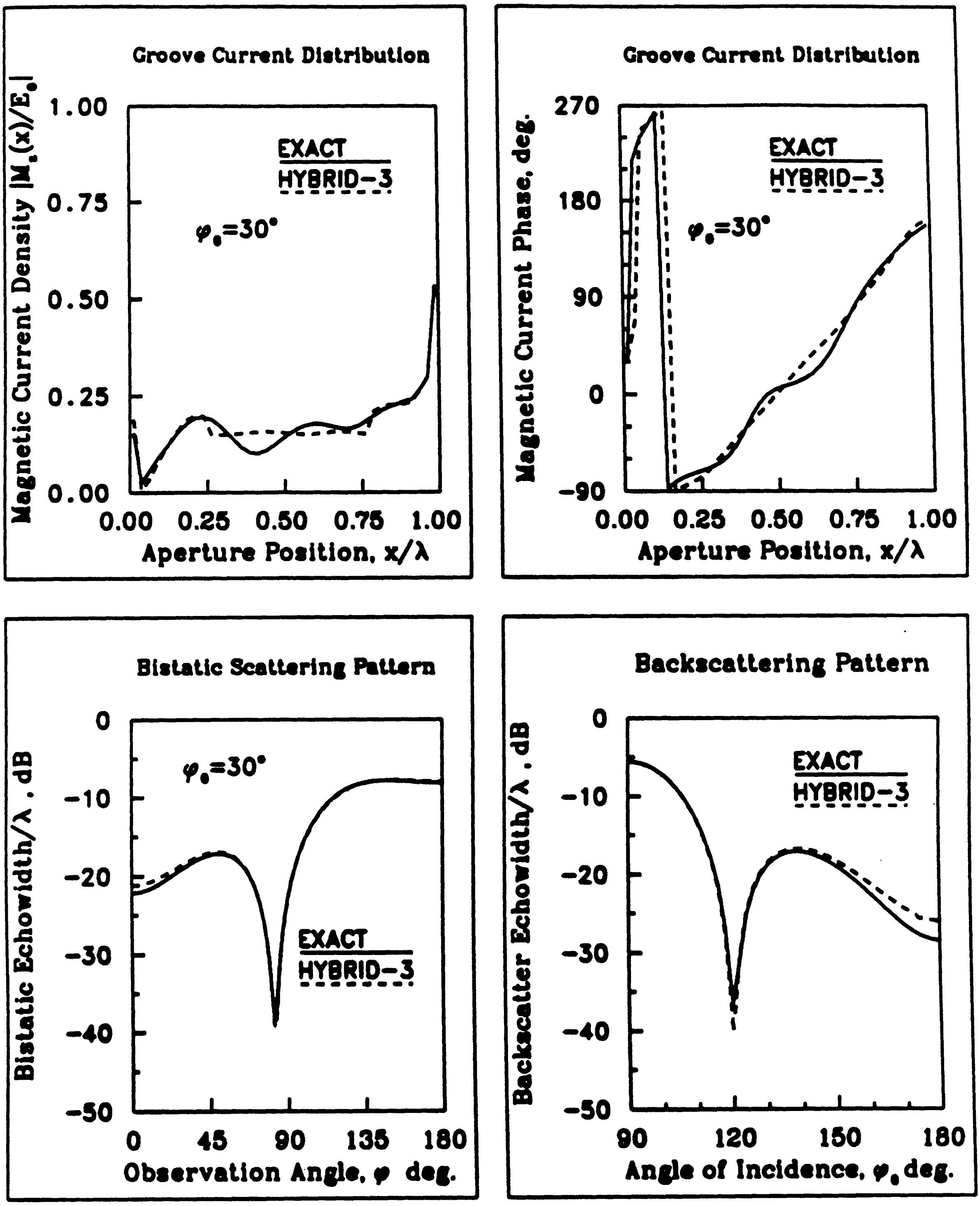

Fig. 5 Comparison of results for scattering from a groove obtained by the exact and the hybrid GIBC formulations; groove width $w=1\lambda$, depth $h=0.2\lambda$, $\epsilon_s=7.0-j1.0$, $\mu_s=1$.

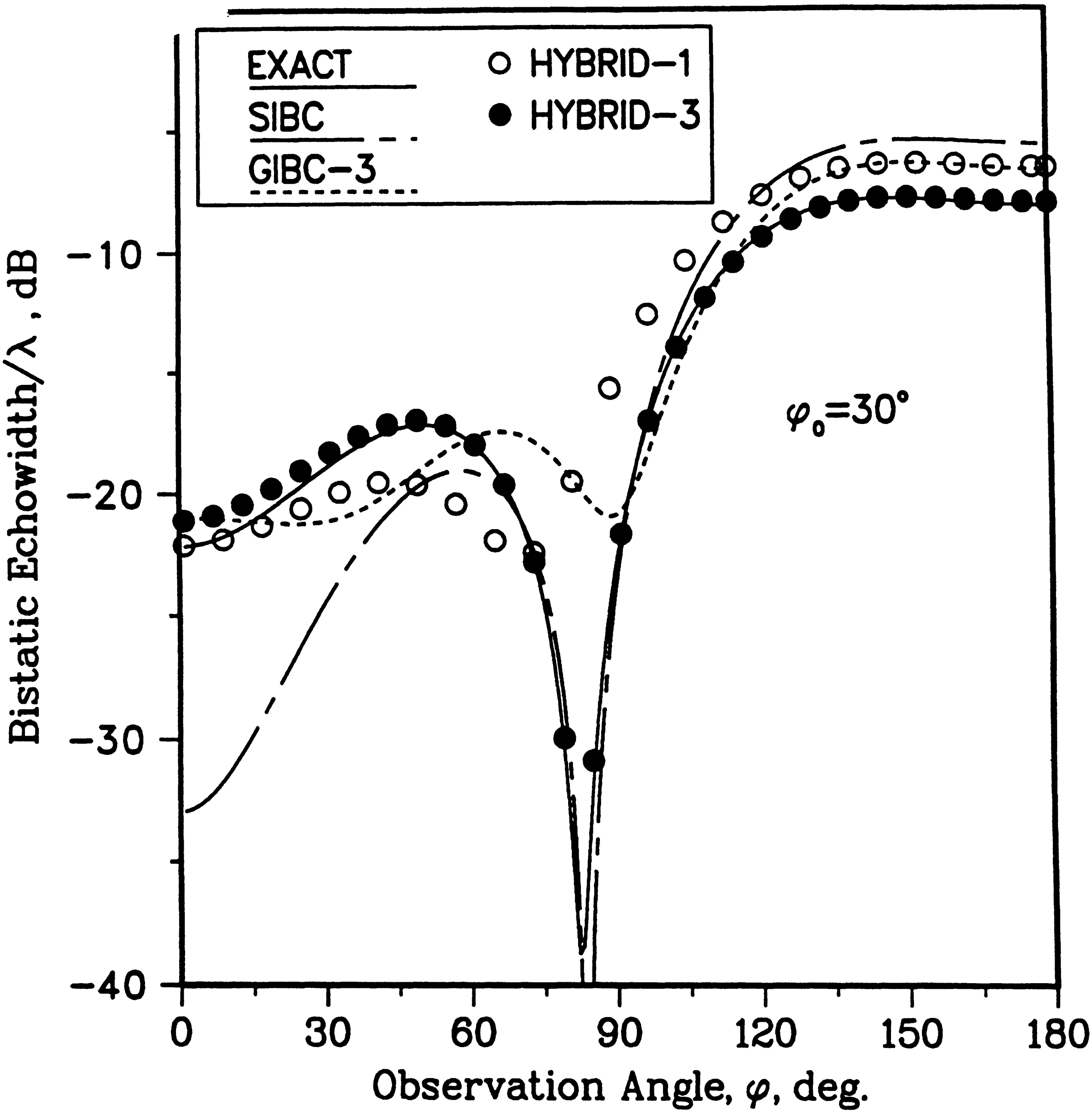

Fig. 6(a) Comparison of bistatic scattering patterns obtained by different formulations as indicated; w=1λ, t=0.2λ, ε_b=7.0–j1.0, μ_b=1.

Scattering from a Dielectric–Filled Groove

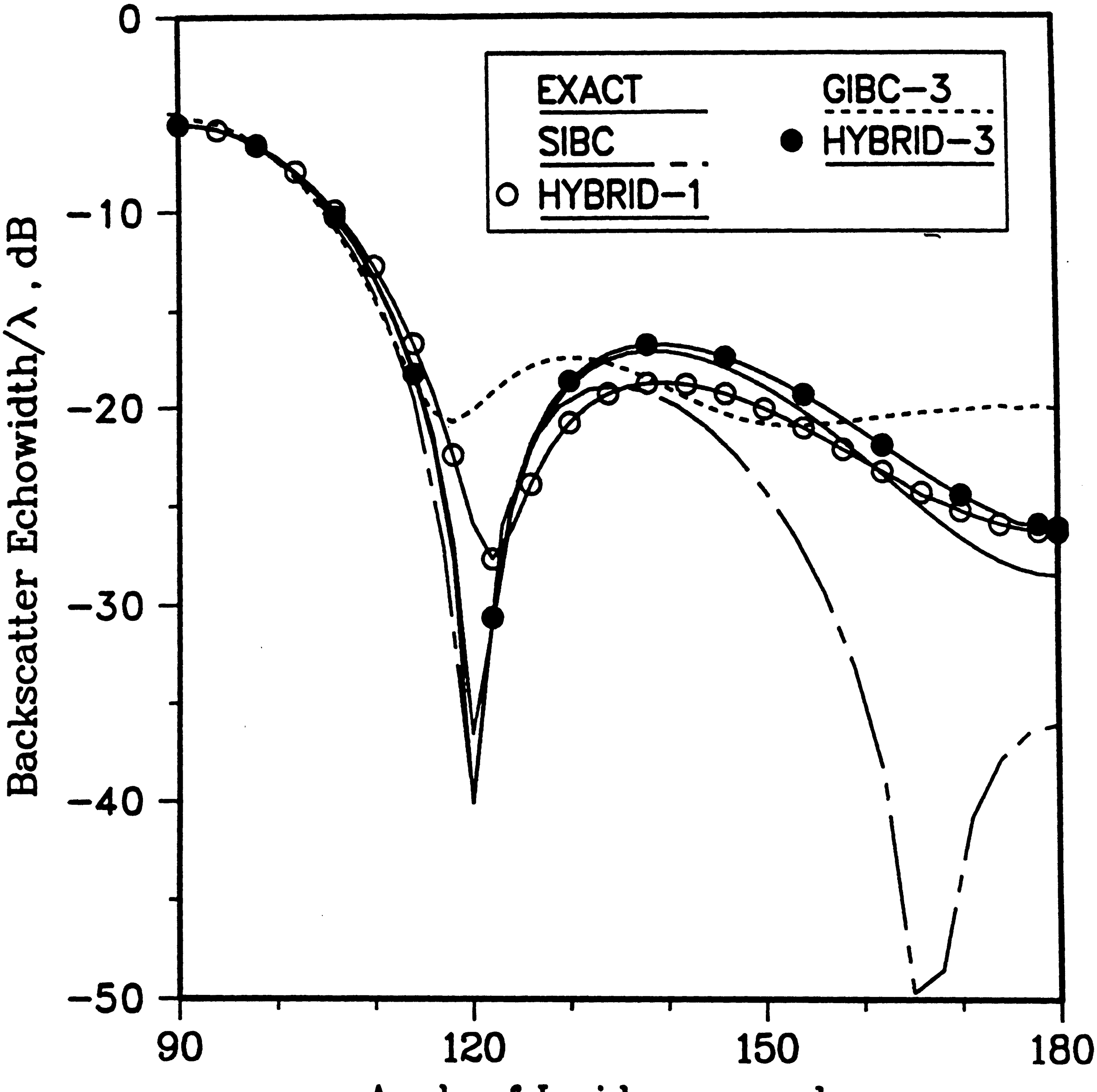

Fig. 6(b) Comparison of backscattering patterns obtained by different formulations as indicated; w=1λ, t=0.2λ, ε_b=7.0−j1.0, μ_b=1.